ELSEVIER

Journal of Alloys and Compounds 330–332 (2002) 14–19

Journal of ALLOYS AND COMPOUNDS

www.elsevier.com/locate/jallcom

Theoretical investigation of Pd–H phase equilibria by the cluster variation method

T. Mohri[a,*], W.A. Oates[b]

[a]*Division of Materials Science and Engineering, Graduate School of Engineering, Hokkaido University, Sapporo 060-8628, Japan*
[b]*Science Research Institute, University of Salford, Salford M5 4WT, UK*

Abstract

By combining the tetrahedron–octahedron approximation of the cluster variation method with a phenomenological expression for the atomic interaction energies, the free energy of the Pd–H system is constructed for both the disordered and chalcopyrite phases. The atomic interaction energies are most conveniently described as the sum of configuration-dependent and -independent contributions. The former originates from chemical atomic interactions while the latter is due to the elastic energy associated with the lattice expansion induced by the dissolution of hydrogen. In the high temperature region, the experimentally observed miscibility-gap type phase diagram is reproduced. The phase separation is caused by the configuration-independent elastic energy contribution. The temperature dependences of the grand potentials of disordered and chalcopyrite phases indicates that an order–disorder transition takes place at 216 K at ~50 at% with weakly second order. The stabilization of the ordered phase is due to the configuration-dependent energies. The site occupancies of hydrogen in the chalcopyrite phase, which consists of two sublattices, α and β, are investigated. It is confirmed that only one of the two sublattices is predominantly occupied by hydrogen at low temperature. Four kinds of independent nearest neighbor pair correlations are calculated and the higher order correlations, including distant pair and multibody correlations, are obtained.

Keywords: Pd–H phase equilibria; Cluster Variation Method; Cluster Expansion Method; Site occupancy; Site correlation

1. Introduction

Based on neutron diffraction and electron channeling studies, it has been revealed that hydrogen atoms occupy the octahedral interstitial sites in Pd [1,2]. As shown in Fig. 1 in which the large and small circles indicate, respectively, Pd atoms and octahedral interstitial sites, the octahedral interstitial sites themselves form a fcc lattice. Hence, to a good approximation, the phase equilibrium for Pd–H can be reduced to that of considering only the H–Vacancy (hereafter abbreviated as Va) subsystem in the fcc lattice surrounded by Pd atoms.

For the Pd–H system, the high temperature portion of the phase equilibria is well established and the various experimental results indicate a miscibility gap due to phase separation [3]. Based on both experimental and theoretical investigations [4–10], it has been revealed that the phase separation is caused by an indirect H–H interaction which is the long range elastic interaction originating from the lattice expansion due to the absorption of hydrogen.

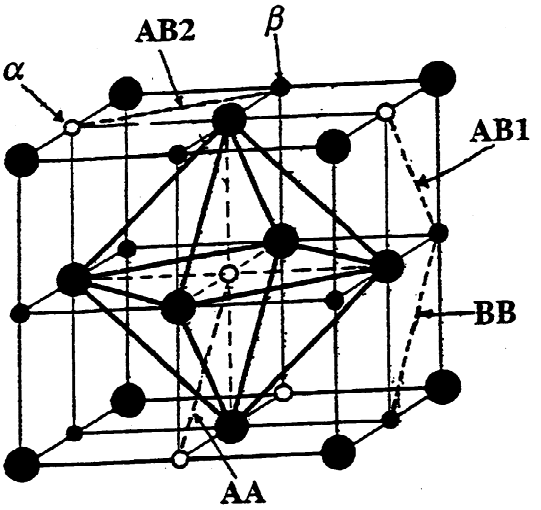

Fig. 1. A unit cell of a fcc lattice and octahedral interstitial sites. A large black circle indicates a Pd atom while small circles are octahedral interstitial sites forming a fcc lattice. When the fcc unit cell formed by interstitial sites are doubled, white and black small circles form a sublattice points, α and β of a Chalcopyrite structure. Four kinds of distinguishable pairs are indicated by AA, AB1, AB2 and BB.

*Corresponding author.
E-mail address: tmohri@eng.hokudai.ac.jp (T. Mohri).

0925-8388/02/$ – see front matter
PII: S0925-8388(01)01663-2

In fact, as has been discussed previously, the non-monotonic variations of excess enthalpy, H_H^E, and entropy, S_H^E, with concentration which were experimentally assessed [11] for the Pd–H system suggest the significance of such an interaction between hydrogens. Yet, a detailed analysis of the excess thermodynamic quantities also indicates the existence of interactions between hydrogen and Va with the same order of magnitude. Such an interaction between *unlike pairs* is expected to induce ordering reactions in the low temperature region and this expectation is confirmed by the observation of a broad (1, 1/2, 0) superlattice reflection in single crystal neutron diffraction experiments. For a recent review of the experimental results on this '50 K anomaly' (see Ref. [20]).

Commencing with the classic work of Lacher [21], there have been many previous attempts at a theoretical calculation of the high temperature miscibility gap part of the Pd–H phase diagram but, to our knowledge, only Ross and co-workers [22,23] have attempted to model both the phase separation and ordering reactions. By using first ($V_{2,1}$) and second ($V_{2,2}$) neighbour pair interaction energies with $V_{2,2}=0.25V_{2,1,}$ Bond and Ross [22] showed, in a Monte Carlo calculation, how the essential features of the observed low temperature ordering part of the phase diagram could be reproduced. Later, Picton et al. [23] extended these calculations to cover both high and low temperature regions by adding on a long-range interaction which was assumed to decrease linearly with H concentration.

In this work we have adopted a somewhat different approach which uses the cluster variation method [13] (hereafter CVM) for the calculation of the configurational-free energy and which utilises a more realistic separation of the total internal energy into configuration-dependent and -independent contributions. Recently, we have shown how this approach can successfully reproduce the high temperature portion of the phase diagram [12] and the main objective of the present investigation was to explore the low temperature portion of the phase diagram *using the same energy parameters employed in the calculation for the high temperature portion*. In this way, we hoped to obtain a description of both the high and low temperature regions within a single theoretical framework.

The power of the CVM is its ability to incorporate a wide range of atomic correlations which play an essential role in the order–disorder transition through pair and multisite correlation functions [14,15] in the free energy formula. The optimized correlation functions provide detailed information of the atomic configurations beyond a single site occupation. This is by no means accessed by a simple lattice gas model. The major focus of the present study is placed in the vicinity of the 1:1 stoichiometric composition for which the *chalcopyrite* type ordered phase is expected to be stabilized. The present study determines not only the preferential site of hydrogen (single site correlation) but also pair and many body site correlations. Such information of higher order atomic correlations should be essential in clarifying the occupation and diffusion mechanisms of hydrogen, which provides the basic knowledge in developing high storage hydrogen materials. The organization of the present report is as follows. In the next section, the theoretical back ground is described. The major results are presented in the third section together with a brief discussion.

2. Theoretical background

2.1. Energetics

In the present study, the total energy is obtained from the experimental measurements [11] of relative hydrogen chemical potential $\Delta\mu_H^\circ$ over a wide temperature range,

$$\Delta\mu_H^\circ = \lim_{r\to 0}\left\{RT\cdot\ln\left[\left(\frac{r_m - r}{r}\right)p_{H_2}^{1/2}\right]\right\} \quad (1)$$

where R is the gas constant, T the temperature, p_{H_2} the hydrogen pressure, r the hydrogen/metal ratio defined as $r = x_H/x_{Pd}$ with $x_H(x_{Pd})$ the concentration of hydrogen (Palladium) and r_m is the chosen maximum value of r. It is noted that $\Delta\mu_H^\circ$ refers to the infinitely dilute solution and is related with partial excess chemical potential μ_H^E through,

$$\mu_H^E = RT\cdot\ln\left[\left(\frac{r_m - r}{r}\right)p_{H_2}^{1/2}\right] - \Delta\mu_H^\circ \quad (2)$$

Since the relative partial enthalpy is given as

$$\Delta\bar{H}_H = R\cdot\frac{\partial\ln p_{H_2}^{1/2}}{\partial\left(\frac{1}{T}\right)} \quad (3)$$

the integration provides the relative integral enthalpy as

$$\Delta H_H = \int_o^r \Delta\bar{H}_H\cdot dr \quad (4)$$

which is regarded here as also being the total internal energy of the system, ΔE, to be employed for the theoretical calculation. Note that both μ_H^E and $\Delta\mu_H^\circ$ can be separated into enthalpic and entropic contributions.

In the present study, the internal energy is most conveniently expressed as the sum of two contributions in the following way [12],

$$\Delta E = E_{NC} + E_C \quad (5)$$

where E_{NC} and E_C are, respectively, configuration-independent (non-configurational) energy and configuration-dependent (configurational) energy. The former is due to the elastic energy contribution originating from the expansion of the Pd lattice caused by the absorption of hydrogen. Continuum elasticity theory [16] is utilized to determine

the non-configurational energy contribution in a series expansion of concentration as follows,

$$E_{\mathrm{NC}}(r,T)=\sum_{i=0}^{i_{\max}} a_i(T)\cdot \xi_1^i \tag{6}$$

where the point correlation function, ξ_1, is linearly related to the concentration, r, through $r=(1/2)\cdot(1+\xi_1)$, and the coefficient term $a_i(T)$ is further expanded in terms of temperature, T, as

$$a_i(T)=\sum_{n=0}^{n_{\max}} b_n\cdot T^n \tag{7}$$

It was demonstrated [11] that a satisfactory fitting is achieved with $i_{\max}=4$ and $n_{\max}=5$ over the temperature range of $T=100$–600 K.

The origin of the configuration-dependent energy stems from chemical interactions among the hydrogen atoms and vacancies and these are regarded as short ranged interactions. The description of the chemical interaction energy can be most efficiently carried out in the framework of the Cluster Expansion Method [17] (hereafter CEM) in the following way,

$$E_{\mathrm{C}}(\{\xi_i\},T)=\sum_i v_i\cdot\xi_i \tag{8}$$

where v_i and ξ_i are the effective interaction energy and correlation function for a cluster specified by subscript i. The correlation function, ξ_i, is defined as the ensemble average of the spin operator $\xi_i=\langle\sigma_{p_1}\cdot\sigma_{p_2}\cdot\cdot\cdot\sigma_{p_i}\rangle$, where σ_p is the spin operator and takes either $+1$ or -1 for H and Va, respectively. Note that the point correlation function is equivalent to the concentration, which guarantees the linear relationship mentioned above.

The key of the CEM is that a set of correlation functions provides an orthonormal basis in the thermodynamic configuration space and the coefficient terms $\{\nu_i\}$ are uniquely determined. The conventional ingredient for determining the effective interaction energies is to operate the CEM on a selected set of ordered compounds for which the total energies are calculated from electronic structure calculations. In the present study, however, *trial-and-error* method is employed on an extracted configurational energy E_{C}. A well educated guess determined that $v_{2,1}=6.08\times10^{-2}$ Ryd, $v_{2,2}=7.599\times10^{-4}$ Ryd and $v_{3,1}=-2.84\times10^{-3}$ Ryd, where $v_{2,i}$ and $v_{3,1}$are, respectively, ith nearest neighbor effective pair interaction and nearest neighbor triangle effective interaction energies. It was confirmed that these values achieve fairly satisfactory fittings over a wide range of temperature and concentration [12].

2.2. Cluster Variation Method

The Cluster Variation Method has been recognized as one of the most powerful theoretical tools for calculating phase equilibria in an alloy system with high accuracy. The level of the approximation depends on the largest cluster selected. In a conventional CVM calculation for fcc-based systems, the tetrahedron cluster is employed as the largest cluster (T approximation), while in the present study the higher order tetrahedron–octahedron approximation [14,15] (hereafter T–O approximation) is employed. This is because the T approximation is unable to incorporate the second nearest neighbor pair interaction energy, $v_{2,2}$, which is not negligible as was indicated above and plays an essential role in stabilizing the underlying ordered phase.

The entropy formula for a disordered solid solution within the T–O approximation is written as

$$S=k_{\mathrm{B}}\cdot\ln\times\frac{\left(\prod_{ijk}(N\cdot z_{ijk})!\right)^8\left(\prod_i(N\cdot x_i)!\right)}{\left(\prod_{ijklmn}(N\cdot v_{ijklmn})!\right)\left(\prod_{ijkl}(N\cdot w_{ijkl})!\right)^2\left(\prod_{ij}(N\cdot y_{ij})!\right)^6} \tag{9}$$

where x_i, y_{ij}, z_{ijk}, w_{ijkl} and v_{ijklmn} are cluster probabilities of finding an atomic arrangement specified by the subscripts on point, pair, triangle, tetrahedron and octahedron clusters, respectively. For an ordered phase, the division of the parent lattice into sublattices increases the number of configurational variables and it is more convenient to employ correlation functions rather than cluster probabilities. It has been demonstrated that the cluster probability and a set of correlation functions are linearly related through

$$X^{\{\delta\}}_{\{J\},n,s}=\frac{1}{2^n}\left\{1+\sum_{n',s',\delta'}V(n,s,\delta;n',s',\delta')\cdot\xi^{\{\delta'\}}_{n',s'}\right\} \tag{10}$$

where $\{J\}$ designates the atomic configuration on a s-type of n-points cluster located on sublattice points indicated by $\{\delta\}$ and $V(n,s,\delta;n',s',\delta')$ is the sum of the product of subscripts in $\{J\}$. It is noted that the sum is taken only for a cluster specified by (n',s',δ') contained in the cluster (n,s,δ). Instead of further providing mathematical formulae, we give an example for tetrahedron cluster probabilities in a chalcopyrite ordered phase which is our main concern of the present study,

$$\begin{aligned}w^{\alpha\alpha\beta\beta}_{ijkl}=\frac{1}{2^4}\{&1+(i+j)\cdot\xi_1^{\alpha}+(k+l)\cdot\xi_1^{\beta}+ij\cdot\xi_2^{\alpha\alpha}\\&+(ik+il+jk+jl)\cdot\xi_2^{\alpha\beta}+kl\cdot\xi_2^{\beta\beta}+(ijk+ijl)\\&\cdot\xi_3^{\alpha\alpha\beta}+(ikl+jkl)\cdot\xi_3^{\alpha\beta\beta}+ijkl\cdot\xi_4^{\alpha\alpha\beta\beta}\}.\end{aligned} \tag{11}$$

Note that, in the actual calculation of Eq. (11), the numbers $+1$ and -1 are assigned to subscripts $i,j,k\ldots$ for H and Va, respectively.

Then, the free energy functional of the system is formulated in terms of a set of correlation functions under a given set of $\{a_i\}$(or $\{b_n\}$) and $\{v_i\}$ in Eqs. (6)–(8). Then,

the equilibrium state of both the phases is determined through

$$\left.\frac{\partial F^{\mathrm{dis}}}{\partial\{\xi_i\}}\right|_{T,\{\xi_{j\neq i}\}} = 0 \tag{12}$$

for a disordered phase and

$$\left.\frac{\partial F^{\mathrm{chal}}}{\partial\left\{\xi_i^{\{\delta\}}\right\}}\right|_{T,\left\{\xi_{j\neq i}^{\delta'}\right\}} = 0 \tag{13}$$

for a chalcopyrite ordered phase. The free energy is further transformed to the *grand potential* by a Legendre transformation and the equality of the grand potential of the two phases determines the phase equilibria.

It is emphasized that the key ingredient of the present study is that the long-range interaction is described in terms only of concentration and is separated out from the short-ranged chemical interaction for which the CVM is used. Thereby, the long-range elastic interaction beyond the basic cluster is tacitly incorporated into the free energy formula.

3. Results and discussion

Shown in Fig. 2 [12] are the concentration dependency of the internal energy, $\Delta E(r)$, at $T=450$ K and its decomposition into non-configurational ($E_{\mathrm{NC}}(r)$) and configurational ($E_{\mathrm{C}}(r)$) energy terms. One notices that both non-configurational and configurational energy contributions are fairly large with opposite signs, which results in the total energy $\Delta E(r)$ having a slightly negative value at this temperature. The opposing tendency of the two contributions indicates that the system drives phase separation reactions at high temperatures where the entropy becomes significant, whereas at low temperatures an ordering reaction takes place due to the large configuration-dependent contribution.

The configuration-dependent energies which were described in the previous section yield the following ratios, $V_{2,2}/V_{2,1}=0.25$ and $V_{3,1}/V_{2,1}=-0.35$, where $V_{2,1}$and $V_{2,2}$ are defined in the Section 1 and $V_{3,1}$ are effective three body interaction energy. Note that $v_{2,1}$, $v_{2,2}$ and $v_{3,1}$ in the previous section are obtained by multiplying $V_{2,1}$, $V_{2,2}$ and $V_{3,1}$, respectively, by the number of corresponding cluster per a lattice point. According to the ground state analysis within the first and second nearest neighbor pair interactions which was performed by Richard and Cahn [18] for fcc-based ordered compounds, three types of ordered phases are possibly stabilized at 1:1 stoichiometry depending upon the ratio of $V_{2,2}/V_{2,1}$which is referred to as the α value. These are $L1_0$, chalcopyrite and $L1_1$ phases for $\alpha\leq 0$, $0\leq\alpha\leq 1/2$ and $\alpha\leq 1/2$, respectively. Therefore, the present results with $\alpha=0.25$ predicts the appearance of the chalcopyrite ordered phase, although the strong three body interaction, $V_{3,1}(v_{3,1})$, demands a careful analysis. The electronic structure calculation performed on Pd–H system by Wang et al. [19] also indicates that chalcopyrite phase is stabilized over other competing ordered phases at the 1:1 stoichiometry. Hence, we focus on the disorder–chalcopyrite phase equilibria in the low temperature portion.

The disorder–order transition temperature is calculated at a constant chemical potential of $\mu=0.0$at which the concentration is nearly fixed at 50 at%. The results of the temperature dependency is shown in Fig. 3. The phase transition temperature, obtained as an intersection (equality) of the two grand potentials, is 216 K and a clear intersection at the transition temperature indicates that the order of the transition is of first order.

A unit cell of chalcopyrite structure is described as the stacking of the two fcc unit cells in the *z*-direction with an antiphase plane inserted in the middle of the cell. One readily understands that the symmetry is different between the *z*-direction and the other two directions (*x*- and *y*-direction). The small circles in Fig. 1, therefore, constitute only one half of the unit cell, and the small white and black circles distinguish the two types of sublattice of the

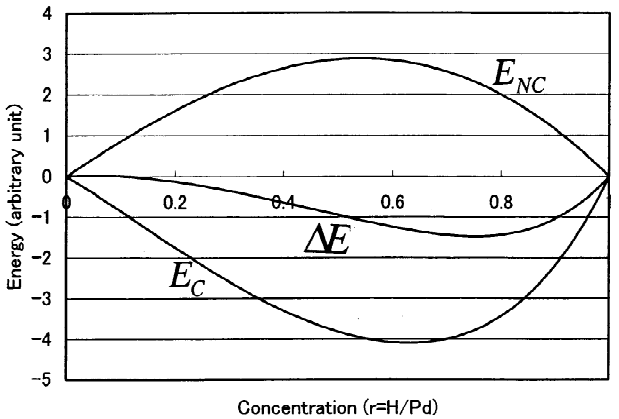

Fig. 2. Concentration variation of internal energy, ΔE, at 450 K and the decomposition to configuration-independent (non-configurational), E_{NC}, and configuration-dependent (configurational), E_{C} contributions. [12].

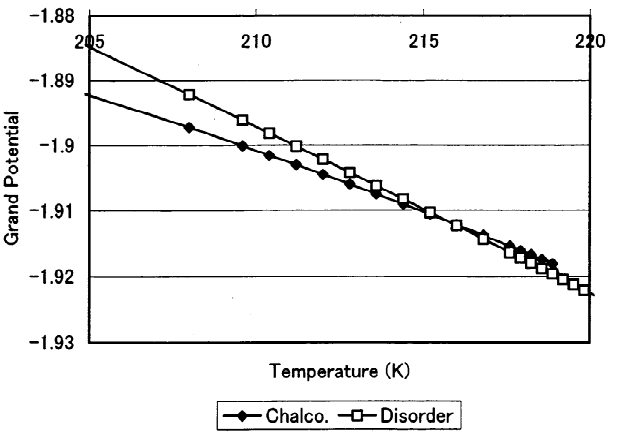

Fig. 3. Temperature variation of grand potentials for chalcopyrite (Chalco.) and disordered (Disorder) phases.

chalcopyrite phase, i.e., α- and β-sublattice points, respectively.

As was mentioned in the previous section, the minimization of the free energy provides a set of correlation functions at an equilibrium state. Substitution of the correlation functions into Eq. (10) provides the equilibrium cluster probabilities. Shown in Fig. 4 is the occupation probability of hydrogen on the α (ALPHA) and β (BETA) sublattices as a function of temperature. The occupation probability is equivalent to the single site cluster probability and corresponds with $X^{\alpha}_{1,1}$ and $X^{\beta}_{1,1}$ which are obtained from the equilibrium values of ξ^{α}_{1} and ξ^{β}_{1}, respectively, through Eq. (10). The concentration of hydrogen(CONC) in the entire lattice is also indicated. The results confirm that a particular sublattice (β) is predominantly occupied in the low temperature range with the two occupation probabilities gradually approaching each other near the transition temperature, finally coinciding at the transition temperature. The discontinuity at the transition temperature is another indication of the first-order transition.

As an example of a higher order site correlation, the pair correlation functions are calculated. It is noted that the symmetry of the chalcopyrite structure requires distinguishing between four kinds of pair cluster. This is because the α−α and β−β clusters are confined in the *z–x* (or *z–y*) plane while the two types of α−β clusters should be distinguished since a α−β pair extends in both *z–x* (*z–y*) and *x–y* directions and these are of different symmetry. Indicated in Fig. 1 are the clusters for AA (α−α), BB (β−β) and AB1 and AB2 (two kinds of α−β), and each probability is shown in Fig. 5. One sees that the predominant pairs are over the β−β sublattice points and the two kinds of α−β pairs are virtually indistinguishable. Again, all the pairs are indistinguishable above the transition temperature merging into ~25% which can be understood since the entire concentration is ~50%.

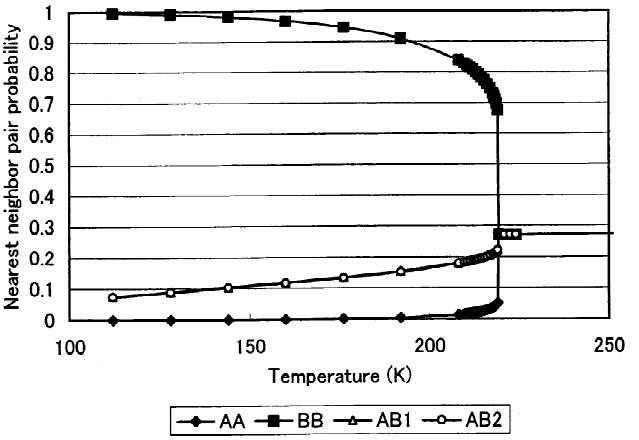

Fig. 5. Temperature dependences of four kinds of nearest neighbor pair cluster probabilities. AA, BB, AB1 and AB2 correspond those in Fig. 1.

Beyond the nearest neighbor pair correlation, one can obtain higher order correlations up to octahedron correlations by the T–O approximation of the CVM. In the present study, however, we simply demonstrate next nearest neighbor pair and triangle cluster probabilities in Figs. 6 and 7. Unlike the case of nearest neighbor pair, the next nearest α−β pairs are confined to the *z–x* (*y*) plane and, therefore, one needs to distinguish only three kinds of pairs. The entire tendency is quite similar to that of nearest neighbor pairs. Although it is not shown explicitly, it is worth mentioning that nearest neighbor and next nearest neighbor pair correlations in the disordered state are opposite in sign, which indicates that the H–Va pair is predominant for the nearest neighbor pair while H–H and Va–Va are dominant for the next nearest neighbor pair. Fig. 7 indicates that a degeneracy of the nearest neighbor triangle configuration for a disordered phase is lifted to two kinds of configuration for a chalcopyrite phase, i.e., α−α−β (3AAB) and α−β−β (3ABB). It is interesting

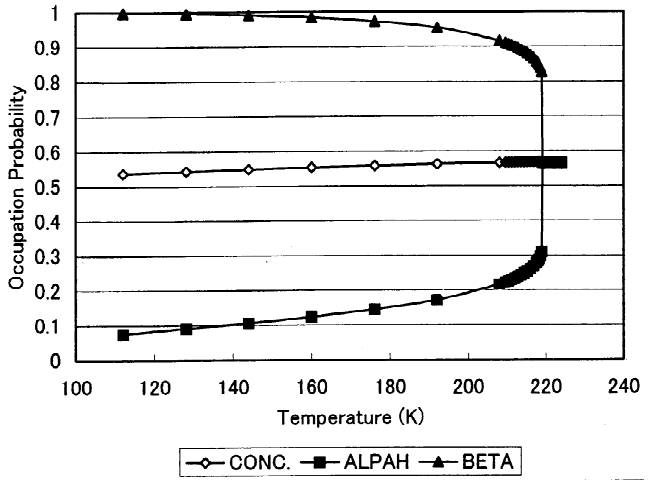

Fig. 4. Temperature dependency of occupation probability for α (ALPHA) and β (BETA) sublattice points in a chalcopyrite structure. The concentration (CONC) of the entire lattice is also indicated.

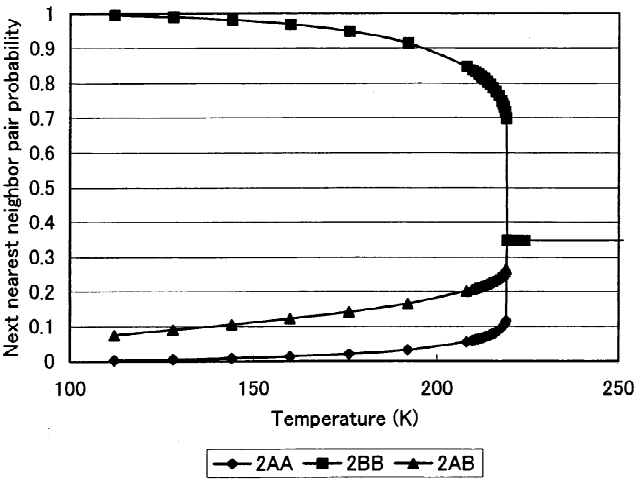

Fig. 6. Temperature dependences of three kinds of next nearest neighbor pair cluster probabilities. 2AA, 2BB and 2AB indicate the next nearest α−α, β−β and α−β pair cluster, respectively.

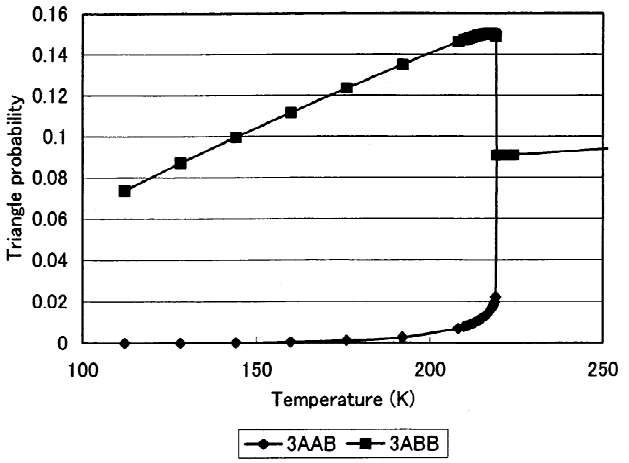

Fig. 7. Temperature dependences of two kinds of nearest neighbor triangle cluster probabilities. 3AAB and 3ABB indicate the nearest neighbor $\alpha-\alpha-\beta$ and $\alpha-\beta-\beta$ triangle clusters, respectively.

that the occupation probability for $\alpha-\alpha-\beta$ increases with temperature towards the transition temperature.

Acknowledgements

This work has been supported in part by a Grant-in-Aid for Scientific Research on Priority Areas A of 'New Protium Function' from the Ministry of Education, Science, Sport and Culture, of Japanese Government.

References

[1] V.A. Somenkov, S.S. Shil'stein, Prog. Mater. Sci. 24 (1980) 267.
[2] I.E. Worsham, M.K. Wilkinson, C.G. Shull, J. Phys. Chem. Solids 3 (1957) 303.
[3] J. Volkl, G. Alefeld, in: A.S. Nowick, J.J. Burton (Eds.), Diffusion in Solids, Recent Development, Academic Press, New York, 1975.
[4] J.R. Lacher, Proc. R. Soc. London Ser. A 161 (1937) 525.
[5] C. Wagner, Z. Phys. Chem. A193 (1944) 386.
[6] E. Wicke, H. Brodowsky, in: G. Alefeld, J. Volkl (Eds.), Hydrogen in Metals, Springer, Berlin, 1978, p. 73.
[7] G. Alefeld, Ber. Bunsenges. Phys. Chem. 74 (1972) 746.
[8] H. Horner, H. Wagner, J. Phys. C 7 (1974) 3305.
[9] S. Dietrich, H. Wagner, Z. Phys. Chem. B36 (1979) 121.
[10] W.A. Oates, A. Stoneham, J. Phys. F13 (1983) 2427.
[11] T. Kuji, W.A. Oates, B.S. Bowerman, T.B. Flanagan, J. Phys. F: Met. Phys. 13 (1983) 1785.
[12] T. Mohri, W.A. Oates, Phil. Mag. (in press).
[13] R. Kikuchi, Phys. Rev. 81 (1951) 988.
[14] J.M. Sanchez, D. de Fontaine, Phys. Rev. B17 (1978) 2926.
[15] T. Mohri, J.M. Sanchez, D. de Fontaine, Acta Metall. 33 (1985) 1171.
[16] J.D. Eshelby, Solid State Phys. 3 (1956) 79.
[17] J.W.D. Connolly, A.R. Williams, Phys. Rev. B27 (1983) 5169.
[18] (a) M.J. Richard, J.W. Cahn, Acta Metal. 19 (1971) 1263;
(b) S.M. Allen, J.W. Cahn, Acta Metal. 20 (1972) 423.
[19] Y. Wang, S.N. Sun, M.Y. Chou, Phys. Rev. B53 (1996) 1.
[20] E. Wu, S.J. Kennedy, E. Mac, A. Gray, E.H. Kisi, J. Phys. Condens. Matter 8 (1996) 2807.
[21] J.R. Lacher, Proc. R. Soc., Ser. A 161 (1937) 52.
[22] R.A. Bond, D.K. Ross, J. Phys. F: Met. Phys. 12 (1982) 597.
[23] D.J. Picton, R.A. Bond, B.S. Bowerman, D.K. Ross, D.G. Witchell, I.S. Anderson, C.J. Carlile, J. Less-Common Metals 88 (1982) 133.